

Unprecedented rock-salt ordering of A and B cations in the double perovskite $\text{Nd}_{2-x}\text{Ca}_x\text{MgTiO}_{6-\delta}$ and defect association

M. Teresa Azcondo,^{a,*} Khalid Boulahya,^b Clemens Ritter,^c Flaviano García-Alvarado^a and Ulises Amador^a

^a Universidad San Pablo-CEU, CEU Universities, Facultad de Farmacia, Departamento de Química y Bioquímica, Urbanización Montepríncipe, Boadilla del Monte, E-28668, Madrid, Spain.

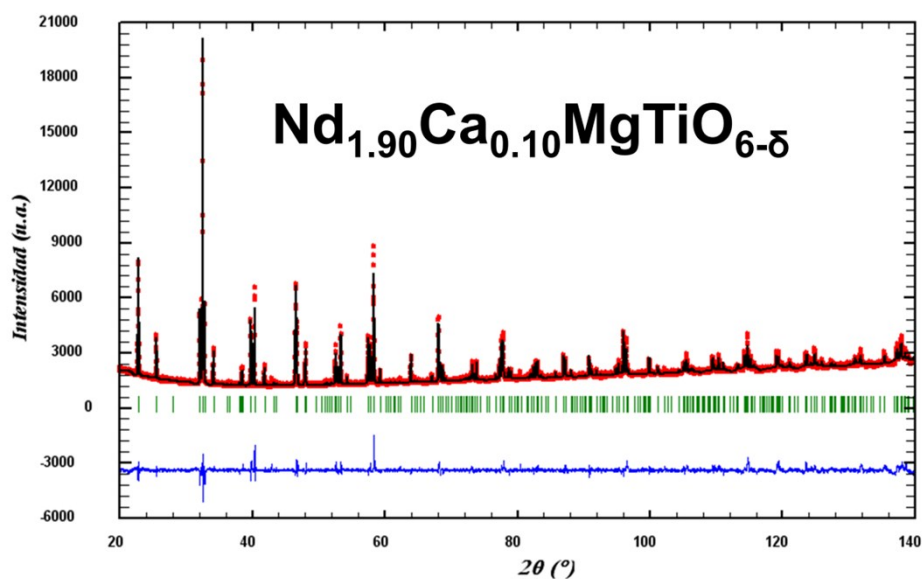
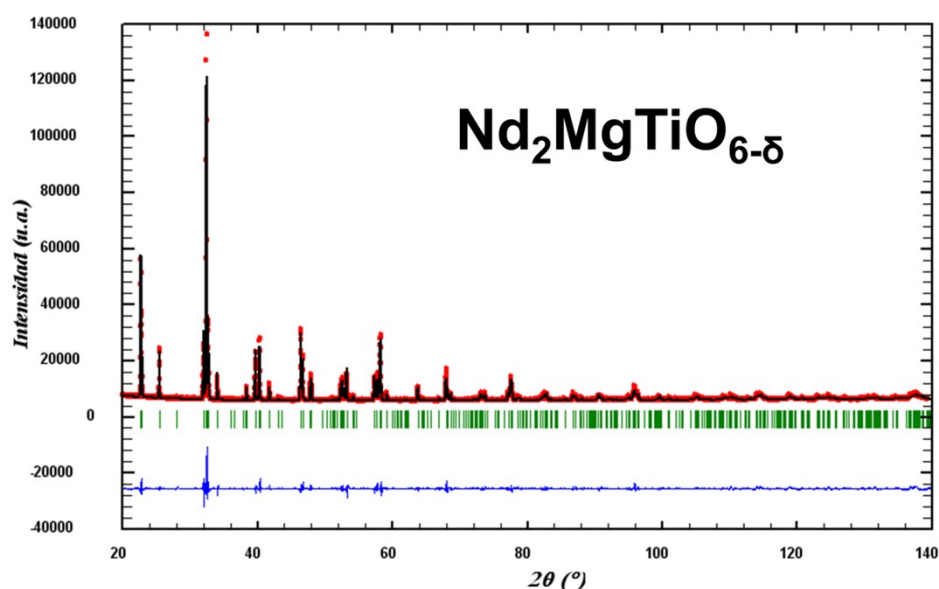
^b Departamento de Química Inorgánica, Facultad de Química, Universidad Complutense, E-28040 Madrid, Spain.

^c Institut Laue-Langevin, BP 156-38042 Grenoble Cedex 9, France.

* e-mail: azcondo@ceu.es

Phone: (34) 91 372 47 15

Fax: (34) 91 351 04 96.



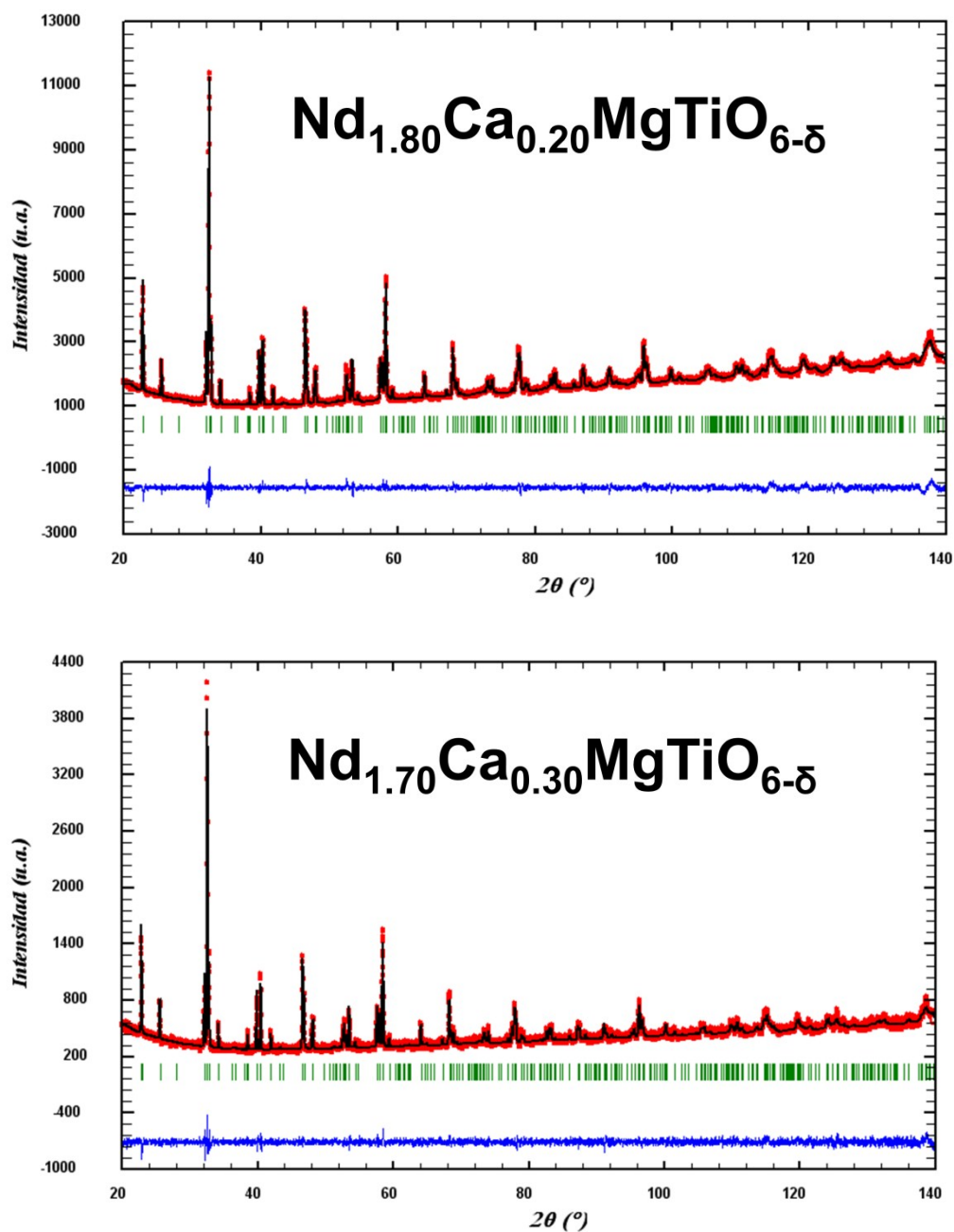


Figure SI 1. Experimental (red circles) and calculated (black continuous line) XRD patterns (and their difference, blue line at the bottom) for samples of the series $\text{Nd}_{2-x}\text{Ca}_x\text{MgTiO}_{6-\delta}$ with ($x=0, 0.10, 0.20$ and 0.30) prepared in air. Vertical bars indicate the positions of the Bragg peaks of the identified phases contained in the sample.

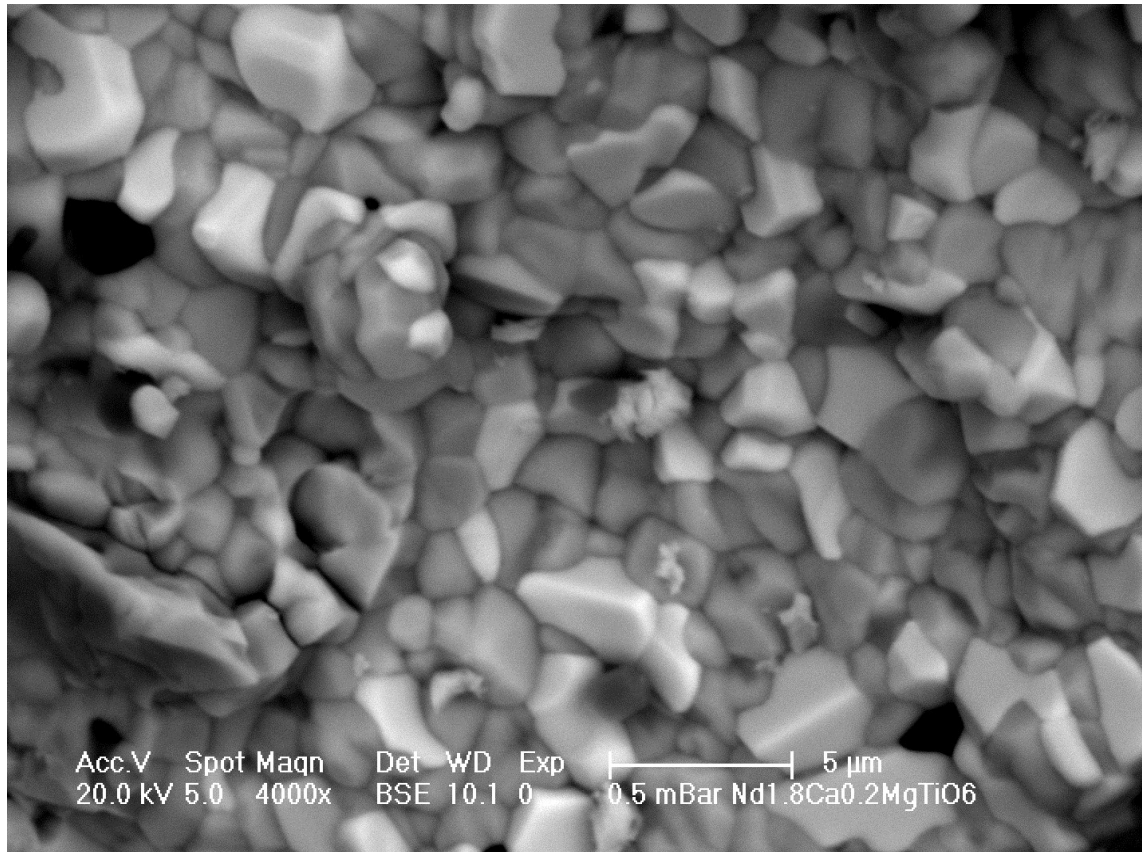


Figure SI 2: Back-scattered electrons (BSE) image taken at a magnification of x 4000 on a sample of composition $\text{Nd}_{1.80}\text{Ca}_{0.20}\text{MgTiO}_{6-\delta}$. Segregation of two different phases is evident as revealed by their different contrasts.

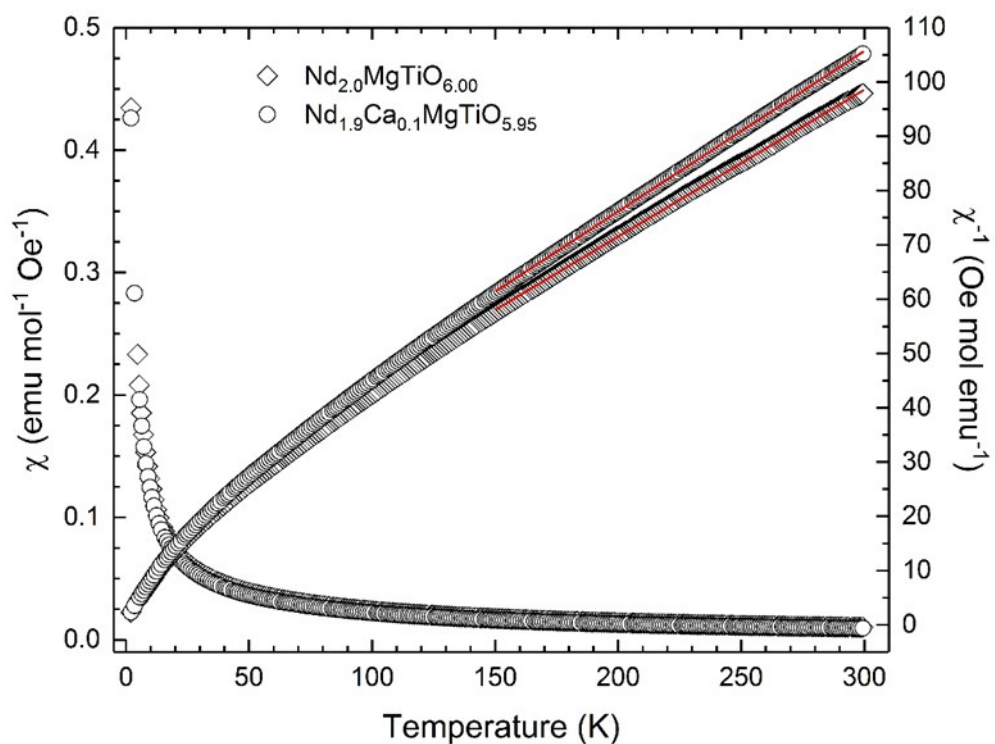


Figure SI 3. Temperature dependence, in an applied magnetic field of 100 mT, of the molar magnetic susceptibility and its inverse for $\text{Nd}_2\text{MgTiO}_6$ (circles) and $\text{Nd}_{1.9}\text{Ca}_{0.1}\text{MgTiO}_{5.95}$ (diamonds) compounds. The solid red lines correspond to the fits of χ^{-1} data from RT to 150 K to the inverse of the Curie-Weiss law.

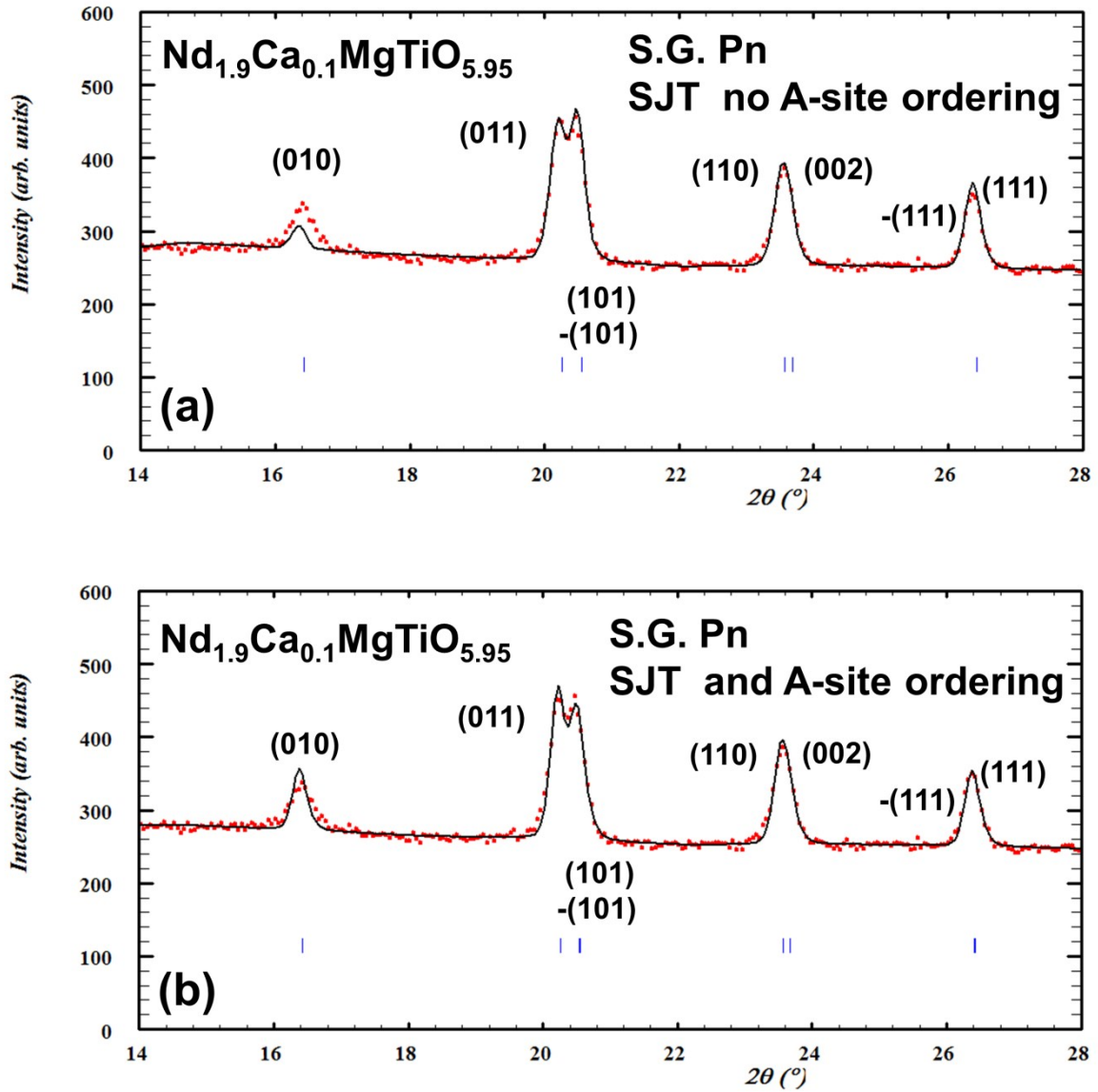


Figure SI 4. Enlargement of the low-angle zone of the NPD data of $\text{Nd}_{1.9}\text{Ca}_{0.1}\text{MgTiO}_{5.95}$ fitted to a structural model with Pn S.G. due to the loss of symmetry (from $P2_1/n$ to Pn) associated to (a) only the second-order Jahn-Teller effect (SJT) due to tetravalent titanium and (b) the combined effect of SJT and rock-salt ordering of A-ions. Note that the intensity of the (010) Bragg peak, forbidden in the S.G. $P2_1/n$ of the parent (un-doped) material, is much better accounted for with the latter model.

Table SI 1. Nominal and experimental (determined by EDS) compositions for the $\text{Nd}_2\text{MgTiO}_{6.6}$ sample used for NPD and electrical characterization.

Element	Nominal composition (atom %)	Experimental composition (atom %)
Nd	20.0	20.6(3)
Mg	10.0	10.3(2)
Ti	10.0	9.5(3)
O	60.0	59.6(3)

Table SI 2. Nominal and experimental (determined by EDS) compositions for the $\text{Nd}_{1.90}\text{Ca}_{0.10}\text{MgTiO}_{6.6}$ sample used for NPD and electrical characterization.

Element	Nominal composition (atom %)	Experimental composition (atom %)
Nd	19.0	19.2(4)
Ca	1.0	1.0(1)
Mg	10.0	10.8(1)
Ti	10.0	10.4(1)
O	60.0	58.6(4)

Table SI 3. Structural parameters for $\text{Nd}_{2-x}\text{Ca}_x\text{MgTiO}_{6-\delta}$ obtained from joint fitting of NPD and XRD data. Agreement factors are given for the fitting of NPD data.

Sample	$x = 0.00^a$				$x = 0.10^b$			
Space Group	$P2_1/n$				Pn			
<i>a</i> (Å)	5.4599(1)				5.4621(1)			
<i>b</i> (Å)	5.5871(1)				5.5791(1)			
<i>c</i> (Å)	7.7681(1)				7.7689(2)			
β (deg)	90.005(1)				90.003(4)			
Volume (Å ³)	236.97(1)				236.75(1)			
A position	4e	O1 position	4e	A' position	2a	O1b position	2a	
Occ Nd	1	X	0.3015(5)	Occ Nd/Ca	0.90(1)/0.10(1)	X	0.786(4)	
X	0.0097(3)	Y	0.2872(4)	X	0.084(4)	Y	0.972(1)	
Y	0.0473(2)	Z	0.9528(4)	Y	0.290(6)	Z	0.141 (4)	
Z	0.7509(3)	Occ	1.000(4)	Z	0.841(4)	Occ	1.002(3)	
U*100 (Å²)	0.03(1)	U*100 (Å²)	0.17(2)	U*100 (Å²)	0.45(7)	U*100 (Å²)	0.29(4)	
B' position	2c	O2 position	4e	A'' position	2a	O2a position	2a	
Occ Mg	1	X	0.2872(5)	Occ Nd/Ca	1.00(1)/0	X	0.366(4)	
U*100 (Å²)	0.55(4)	Y	0.3035(4)	X	0.067(4)	Y	0.553(2)	
B'' position	2d	Z	0.5446(4)	Y	0.1958(6)	Z	0.636(4)	
Occ Ti	1	Occ	0.998(3)	Z	0.340(4)	Occ	1.000(2)	
U*100 (Å²)	0.58(4)	U*100 (Å²)	0.17(2)	U*100 (Å²)	0.06(4)	U*100 (Å²)	0.29(4)	
		O3 position	4e	B' position	2a	O2b position	2a	
		X	0.9126(3)	Occ Mg/Ti	0.127(3)/0.873(3)	X	0.787(4)	
		Y	0.4763(3)	X	0.59047	Y	0.956(1)	
		Z	0.7429(4)	Y	0.262(3)	Z	0.546(4)	
		Occ	1.002(4)	Z	0.09002	Occ	0.998(4)	
		U*100 (Å²)	0.17(2)	U*100 (Å²)	0.01(3)	U*100 (Å²)	0.29(4)	
				B'' position	2a	O3a position	2a	
				Occ Mg/Ti	0.873(3)/0.127(3)	X	-0.007(4)	
				X	0.0912(3)	Y	0.736(1)	
				Y	0.764(2)	Z	0.833(4)	
				Z	0.082(3)	Occ	0.999(3)	
				U*100 (Å²)	0.01(4)	U*100 (Å²)	0.29(4)	
				O1a position	2a	O3b position	2a	
				X	0.387(4)	X	0.164(4)	
				Y	0.555(2)	Y	0.782(1)	
				Z	0.045(4)	Z	0.344(4)	
				Occ	0.945(5)	Occ	1.003(3)	
				U*100 (Å²)	0.29(4)	U*100 (Å²)	0.29(4)	
^a $P2_1/n$ (#14): 4e (xyz), 2c ($\frac{1}{2}$ 0 $\frac{1}{2}$), 2d ($\frac{1}{2}$ 0 0), $\chi^2 = 1.94$, $R_{wp} = 4.31\%$, $R_{exp} = 3.10\%$, $R_B = 2.69\%$, Composition: $\text{Nd}_2\text{MgTiO}_{6.00(1)}$				^b Pn (#7): 2a (xyz) $\chi^2 = 11.0$, $R_{wp} = 3.69\%$, $R_{exp} = 1.11\%$, $R_B = 2.81\%$, Composition: $\text{Nd}_{1.90(1)}\text{Ca}_{0.10(1)}\text{MgTiO}_{5.94(1)}$				

Table SI 4. Selected structural information for $\text{Nd}_{2-x}\text{Ca}_x\text{MgTiO}_{6-\delta}$ ($x=0.00, 0.10$) obtained from NPD data. Angles are given in degrees and distances in Å (up to 3.50 Å); distortion Δ of the BO_n polyhedra and Bond Valence Sums [1], are reported as $\Delta=1/n \sum_{j=1,n} \{(d_n - \langle d \rangle)/\langle d \rangle\}^2$ where $\langle d \rangle$ is the average B-O distance. The quadratic elongation λ is given by $\lambda= \sum_{j=1,n} (l_j/l_0)^2/n$ and the bond-angle variance σ is given by $\sigma = \sum_{j=1,n} (\theta_j - \theta_0)^2/(n-1)$ where l_0 and θ_0 are the cation-anion bond lengths and cation-anion-cation bond angles in regular coordination polyhedra, respectively, and l_j and θ_j are the cation-anion bond lengths and cation-anion-cation bond angles of the i th bond [2]

Nd₂MgTiO_{6.00(1)}		Nd_{1.90(1)}Ca_{0.10(1)}MgTiO_{5.94(1)}			
^a Tilt angle θ	20.05(3)/19.77(4)	^a Tilt angle θ	21.0(1)/17.6(2)		
^b Tilt angle ϕ	20.05(3)/19.77(4)	^b Tilt angle ϕ	21.0(1)/17.7(1)		
^c Tilt angle μ	14.5(1)/14.2(1)	^c Tilt angle μ	15.8(3)/12.5(3)		
TiO₆ octahedron		B'(Mg/Ti)O₆ octahedron			
B'-O(1) x 2	1.970(2)	B'-O1a x 1	2.01(2)		
B'-O(2) x 2	1.945(3)	B'-O1b x 1	1.98(1)		
B'-O(3) x 2	1.951(3)	B'-O2a x 1	1.86(2)		
		B'-O2b x 1	2.08(2)		
		B'-O3a x 1	1.96(3)		
		B'-O3b x 1	1.97(3)		
Average B'-O	1.956(1)	Average B'-O	1.98(1)		
Octahedron volume (Å³)	9.966	Octahedron volume (Å³)	10.262		
Distortion B'-O₆ x 10⁴	0.30	Distortion B'-O₆ x 10⁴	11.2		
Quadratic elongation	1.0003	Quadratic elongation	1.0031		
Bond angle variance	0.6761 deg ²	Bond angle variance	6.7651 deg ²		
BVS	4.11(1)	BVS	3.91(8)		
MgO₆ octahedron		B''(Mg/Ti)O₆ octahedron			
B''-O(1) x 2	2.064(3)	B''-O1a x 1	2.01(2)		
B''-O(2) x 2	2.085(3)	B''-O1b x 1	2.08(2)		
B''-O(3) x 2	2.058(3)	B''-O2a x 1	2.19(2)		
		B''-O2b x 1	1.92(2)		
		B''-O3a x 1	2.01(4)		
		B''-O3b x 1	2.08(4)		
Average B''-O	2.069(1)	Average B''-O	2.05(1)		
Octahedron volume (Å³)	11.7966	Octahedron volume (Å³)	11.4448		
Distortion B''-O₆ x 10⁴	0.31	Distortion B''-O₆ x 10⁴	17.0		
Quadratic elongation	1.0004	Quadratic elongation	1.0035		
Bond angle variance	1.2459 deg ²	Bond angle variance	6.2738 deg ²		
BVS	2.18(1)	BVS	2.33(7)		
NdO_n polyhedron		(Nd/Ca)O_n polyhedron		NdO_n polyhedron	
Nd-O1 x 1	2.606(3)	(Nd/Ca)-O1a x 1	2.73(2)	Nd-O1a x 1	2.33(3)
Nd-O1 x 1	2.383(3)	(Nd/Ca)-O1a x 1	2.68(4)	Nd-O1b x 1	2.51(3)
Nd-O1 x 1	2.740(4)	(Nd/Ca)-O1b x 1	2.40(3)	Nd-O2a x 1	2.38(3)
Nd-O2 x 1	2.629(3)	(Nd/Ca)-O2a x 1	2.66(3)	Nd-O2b x 1	2.59(3)
Nd-O2 x 1	2.368(4)	(Nd/Ca)-O2a x 1	2.73(4)	Nd-O2b x 1	2.72(4)
Nd-O2 x 1	2.716(4)	(Nd/Ca)-O2b x 1	2.38(3)	Nd-O3a x 1	2.36(3)
Nd-O3 x 1	2.456(2)	(Nd/Ca)-O3a x 1	2.54(1)	Nd-O3b x 1	2.37(3)
Nd-O3 x 1	2.341(2)	(Nd/Ca)-O3b x 1	2.33(3)		
Average Nd-O	2.530(1)	Average (Nd/Ca)-O	2.55(1)	Average Nd-O	2.47(1)
BVS	2.75(1)	BVS	2.57(8)	BVS	2.77(9)

^a With [110], ^b With [1-10], ^cWith [001]

[1] Zachariasen, W.H., Acta Crystallographica, 1963. **16**: p. 385.

[2] Robinson, K., Gibbs, G. V. & Ribbe, P. H., Science, 1971. **172**: p. 567-570.

Table SI 5. Curie constant C and Weiss temperature θ values obtained by fitting the inverse of the molar magnetic susceptibility data to the function $\chi^{-1} = \left(\frac{C}{T - \theta}\right)^{-1}$ in the temperature range 150–300 K; and the experimental magnetic moment μ_{exp} values calculated as $\sqrt{8 \times \frac{C}{2 - x}}$

Compound (Nd _{2-x} Ca _x MgTiO _{6-δ})	C (emu K mol ⁻¹ Oe ⁻¹)	θ (K)	μ_{exp} (μ_B per Nd)
Nd ₂ MgTiO ₆ (x=0.00)	3.384±0.004	-64.5±0.5	3.68±0.04
Nd _{1.90} Ca _{0.10} MgTiO _{5.95} (x=0.10)	3.331±0.002	-57.7±0.2	3.65±0.03